Received 15 May 2024, accepted 26 May 2024, date of publication 3 June 2024, date of current version 13 June 2024.
Digital Object Identifier 10.1109/ACCESS.2024.3408955

RESEARCH ARTICLE

Exposure Assessment for Wearable Patch Antenna Array at Millimeter Waves

SILVIA GALLUCCI[1], MARTA BONATO[1], MARTINA BENINI[1,2], MARTA PARAZZINI[1], (Member, IEEE), AND MAXIM ZHADOBOV[3], (Senior Member, IEEE)
[1]Istituto di Elettronica e di Ingegneria dell'Informazione e delle Telecomunicazioni (IEIIT), Consiglio Nazionale delle Ricerche (CNR), 20133 Milan, Italy
[2]Dipartimento di Elettronica, Informazione e Bioingegneria (DEIB), Politecnico di Milano, 20133 Milan, Italy
[3]Institut d'Électronique et des Technologies du numéRique (IETR), CNRS, UMR 6164, University of Rennes 1, 35000 Rennes, France

Corresponding author: Silvia Gallucci (silvia.gallucci@cnr.it)

This work was supported by the European Defence Agency (EDA) through the "Biological Effects of Radiofrequency Electromagnetic Fields (RFBIO)" project funded by the Italian Ministry of Defense (MoD) under Project B 0987 IAP2 GP.

ABSTRACT The upcoming deployment of wireless networks and systems operating in the upper part of the microwave spectrum, including millimeter-wave (mmWave) frequencies, motivates user exposure assessment studies at these emerging frequencies. At mmWaves, the power absorption is mainly limited to cutaneous and subcutaneous tissues. Till now, there is no literature consensus on the skin model to employ in computational exposure assessment studies. For these reasons, this work analyses four different models of the most superficial tissues with different degree of details exposed to wearable patch antennas operating at 28 GHz and 39 GHz. The results for the layered models are compared to the homogeneous one. Simulations were performed using the FDTD method, implemented in the Sim4life platform and the exposure was assessed in terms of the absorbed power density averaged over 1 cm^2 and 4 cm^2 (S_{ab}). The data showed that the homogeneous model underestimates the peak value of S_{ab} obtained for multi-layer models in the stratum corneum (by 8% to 12% depending on the number of layers of the model and the frequency) when the simulated models have the same reflection coefficient. Conversely, there are no substantial differences in the exposure levels between the layered models.

INDEX TERMS Wearable device, computational dosimetry, skin model, millimeter waves.

I. INTRODUCTION

The use of wearable technologies is increasingly growing. They are very attractive for various applications, spreading from healthcare to smart home [1], [2]. The wearable technology is based on the concept of the Body-Area Network (BAN) consisting in a network of sensors/actuators/antennas able to exchange with each other and with an external gateway information about the user's health condition, position, environment and so on [3]. This involves communication between sensors, central BAN unit, and external node, e.g. smartphone, at two levels of communication: intra-BAN and inter-BAN [4]. The communication protocol of the wireless BAN (WBAN) is defined in the IEEE 802.15.6 standard [5] in which several frequency bands are identified. The operating frequencies include the 2.4 GHz Industrial-Scientific-Medical (ISM) band, which became standard for such type of systems due to the spread of the Bluetooth, BLE and Zigbee protocols [6].

Due to the way of use of the wearable devices that entails to pose them at a very short distance from the human body (typically from zero to several mm), the assessment of the human exposure to the electromagnetic field (EMF) emitted by these devices is needed. Indeed, there is increasing public concern regarding safety of new/emerging wireless systems [7].

Due to the increasing use of new frequency bands for 5G and wearables, including millimeter waves (mmWaves), the exposure assessment becomes even more critical. Some studies report the design of novel mmWave wearable antennas addressing the question regarding the human exposure

The associate editor coordinating the review of this manuscript and approving it for publication was Valerio De Santis.

(e.g., [8], [9], [10]) but they appear not to be exhaustive because of the way to model the human skin.

Indeed, since in the upper part of the microwave spectrum the absorbed in the body electromagnetic power is confined in the superficial tissues, the use of an appropriate tissue model is crucial as it directly impacts the reliability and accuracy of results. The spatial resolution of the commonly used computational anatomical human models [e.g.,11] is not fine enough to accurately represent the near-surface tissues at mmWaves. Indeed, in this type of models, the skin is typically modelled as a homogeneous tissue, disregarding its heterogeneous structure [12]. For this reason, stratified multi-layer cutaneous models were introduced [7], [13].

Alekseev et al. [14] derived the dielectric properties of two skin layers at various locations on the body in the 37-78 GHz range: the stratum corneum (SC), the external layer of skin, and the viable epidermis and dermis. In another study [15], the same group compared the absorbed in the body electromagnetic power in the frequency range 30-300 GHz using three stratified skin models: the first one made of dermis, the second one made of SC and viable epidermis and dermis, and the third one based on three layers (SC, viable epidermis and dermis, and fat). In this study, the authors also investigated the impact of the skin thickness depending on the on-body location. Indeed, the thickness of the outermost layer of the skin, i.e. SC, depends on the anatomical region, which can be broadly classified into body regions with thin SC (e.g. forearm, 10-20 μm) and regions with thick SC (e.g. palm, 20-700 μm). The results demonstrated that there are no significant differences between the power density and specific absorption rate (SAR) in the two multi-layer models, both with thick SC (0.43 mm). Sasaki et al. [16] used a skin model where viable epidermis and dermis were modelled as two separate layers and followed by a subcutaneous adipose tissue (SAT) and a muscle layer. By means of Monte Carlo method they showed that, for a plane wave at frequencies ranging from 10 GHz to 1 THz, the skin thickness affects the electromagnetic power absorption. Sacco et al. [17] considered the age-dependent variations of the skin permittivity and thickness. The models consisted of four layers: SC, viable epidermis and dermis, fat, and muscle. The results showed that the skin thickness affects more the power density and SAR in lower mmWave bands (i.e., 26 GHz) and in particular for people $<$ 25 years old; in general, considering both the thickness and the transmission coefficient variations demonstrates an increase of the power absorption with age for both the considered frequencies. Christ et al. [18] focused on the power reflection coefficient and the temperature increase induced in a five-layered model: SC, viable epidermis, dermis, fat, and muscle. The results showed that the homogeneous model underestimates more than by a factor of three the induced temperature increase with respect to the layered one, when the frequency (6-100 GHz) of the plane wave and the thicknesses of SC (10-700 μm) are varied. Later, Christ et al. [19] demonstrated that the homogeneous model with electromagnetic properties of dermis underestimates the power transmission coefficient at the air/skin interface (T(θ), where θ is the incidence angle of the plane wave) when compared to the multi-layer model made of thick SC, viable epidermis and dermis, fat, and muscle (plane wave, 6-300 GHz), whereas there is no evident difference in terms of power transmission coefficient T(θ) between the homogeneous model and the multi-layer one with thin SC. Finally, Ziskin et al. [13] calculated the reflection coefficient, the power deposition and the temperature increase in two different skin models: three- and four-layered ones. The models were analyzed with an incident plane wave at 37-78 GHz and the results obtained by means of both the analytical and the computational approaches revealed that the power absorption mainly occurs in the most superficial layers, as expected. Models also including the inner tissues (i.e., fat and muscle) are more relevant for the thermal analysis since the heat propagates deeper compared to the EMF.

In light of the above-mentioned literature studies, it is clear that there is no literature consensus on the skin modeling approach to employ in computational exposure assessment studies. In their recent review paper, Hirata et al. [7] reaffirmed the importance of using appropriate human models because the improvement of their degree of details can make the results obtained by means of the computational approach even more reliable. This is valid especially at mmWaves, where a realistic representation of the skin structure could strongly impact the exposure assessment.

In addition, even the international organizations setting the exposure limits do not refer to a standard tissue model for the power density computation. Indeed, the ICNIRP guidelines [20], where the exposure limits are mainly set based on the EMF-induced heating in human, refer to the absorbed power density as a dosimetric quantity at frequencies $>$ 6 GHz without defining neither which is the appropriate model to reproduce the skin, nor which is the skin layer to be considered for the comparison with the exposure limits. On the other hand, IEEE Std. C95.1 [21] suggests using the epithelial power density as the dosimetric reference quantity between 6 GHz and 300 GHz, "epithelial" referring to the SC for the skin. Finally, concerning the introduction of the absorbed power density (APD/S_{ab}) as a new metric of interest for assessing exposure to EMF above 6 GHz, several studies have been reported in the literature. For example, some of these studies rely on estimating peak spatial-averaged APD for the spatial SAR distribution [22], [23], while others focus on calculating APD through comparing various numerical methods [24], [25]. Still, others investigate how the irregular geometry of the field-exposed surface may impact the APD calculation.

For all these reasons, further investigations are needed with the aim to deepen the variation on the exposure results owing to the employed approach for the cutaneous tissue modelling. The literature is lacking exposure assessment studies involving skin models with different stratifications at mmWave frequencies and, particularly, to wearable antennas. Indeed, the majority of the studies identify an incident plane wave as an electromagnetic field (EMF) source, thus ignoring antenna/body interactions and simplifying the studied scenario.

The main objective of this study is to analyze and compare in terms of APD models of the superficial tissues with different stratification and degree of details when they are irradiated with an EMF emitted by two wearable antennas, tuned to a specific frequency dedicated to the 5G technology. The analysis is performed for two wearable patch antenna arrays in 5G FR2 bands (i.e., 28 GHz and 39 GHz). This allowed us to investigate the impact of the degree of stratification of the near-surface tissues models on the dosimetric quantities. Four multi-layer models with increasing complexity are considered: from a homogeneous with dermis properties to the four-layered model composed of the SC, dermis, fat, and muscle. For each model, the absorbed power density is computed (FDTD method) and analytically calculated for an incident plane wave varying the angle of incidence (θ).

II. MATERIALS & METHODS

In this section, first the geometrical and electromagnetic properties of the tissue models are introduced. Then antenna design is presented, followed by the description of the numerical method and analytical approach.

A. ANATOMICAL MODELS

We considered four superficial tissue models of increasing complexity: (i) homogenous single layer with dermis properties, (ii) two-layered, made of SC and dermis, (iii) three-layered made of SC, dermis, and fat, (iv) four-layered, modelled as SC, dermis, fat, and muscle [16]. The dielectric properties of each layer (Table 1) were chosen according to the literature data at 30 GHz and 40 GHz [13], [18] and here assigned to 28 GHz and 39 GHz, respectively.

The ranges of thickness of each layer were taken from the literature [13], [18]. In particular, the range of thicknesses of the SC was chosen in the range of dry "thin skin" because most of the body regions belong to it, except the palms and the soles of feet. Table 2 reports the thicknesses used corresponding to the typical thicknesses of fat, muscle, and viable epidermis and dermis; the thickness of the SC corresponds to the minimum value of the range of the "thin skin". This value was found to be the best option in order to minimize the differences between the reflection coefficient (Γ) of each multi-layer model, as shown in Fig.1. This figure reports the reflection coefficient $|\Gamma|$ for a plane wave at 28 GHz impinges on each multi-layer models. The incidence angle (θ) varies from 0° up to 80°. For the TM polarization, $|\Gamma|$ decreases down to the Brewster's angle which is approximately at the limit of 80°. For the TE polarization, $|\Gamma|$ monotonically increases with θ. A comparable trend was detected also for a plane wave at 39 GHz.

The overall dimension of the models is 150 × 150 mm, and the depth was chosen to be thick enough in order to avoid contribution from the reflection at the deepest interface.

B. ANTENNAS

The wearable antennas have to comply with constraints in terms of compact size, lightness, and low profile [27]. To satisfy the aforementioned requirements, the two simulated antennas, inspired from Chahat et al. [28] and redesigned at 28 GHz and 39 GHz, are microstrip-fed four-patch antenna arrays (Figure 2). They consist of three layers: ground plane, radiative element, and RT Duroid 5880 substrate ($\varepsilon_r = 2.2$, $\sigma = 5{\cdot}10^{-4}$S/m). The overall antenna dimensions and inter-element distances are chosen to resonate at 28 GHz and 39 GHz (Table 3).

TABLE 1. Properties at 28 GHz and 39 GHz.

Tissue	Relative Permittivity (ε_r)		Conductivity (σ) [S/m]		Density (ρ) [kg/m^3]
	28 GHz	39 GHz	28 GHz	39 GHz	
Stratum Corneum (SC)	3.52	3.33	1.21	1.44	1500
Viable Epidermis & Dermis	16	12.1	27.5	32.6	1109
Fat	3.42	3.1	2.32	2.68	911
Muscle	21.5	15.6	39.9	47.1	1090

TABLE 2. Thicknesses of layers [mm].

Tissue	Homogeneous	2-Layered Model	3-Layered Model	4-Layered Model
Stratum Corneum (SC)	-	0.01	0.01	0.01
Viable Epidermis & Dermis	∞	∞	0.96	0.96
Fat	-	-	∞	1.6
Muscle	-	-	-	∞

C. COMPUTATIONAL APPROACH

The exposure was assessed for the antenna located 2 mm from the tissue model. The scenario is represented in Fig. 3 where the dimensions of the antenna and the phantom are not in scale, indeed, the size of the phantom is considerably greater than the one of the antennas, with the antenna that covers only the 6% of the surface of the human phantom. The exposure scenario was the same for both antennas and the accepted power was set in both cases to 100 mW.

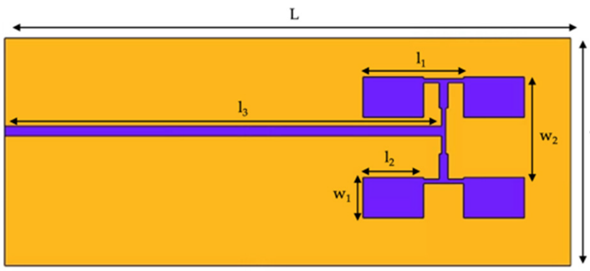

FIGURE 1. The geometry of simulated wearable antennas.

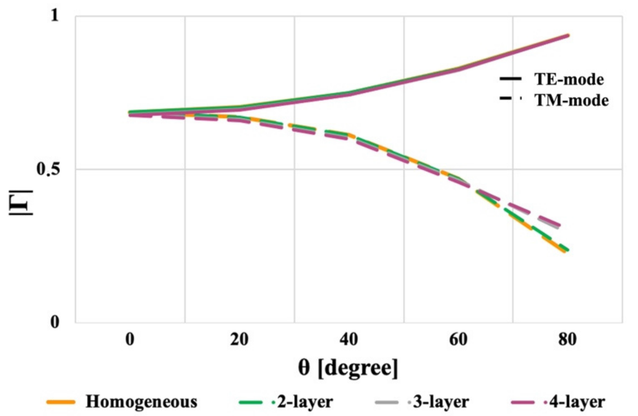

FIGURE 2. Reflection coefficient at 28 GHz at the air/phantom for each of the simulated tissue models.

TABLE 3. Antenna dimensions [mm].

Values	Dimensions	
	28 GHz	39 GHz
L	40	33.5
W	16.62	13.6
l_1	9.6	6
l_2	5	3.6
l_3	30.25	25.88
w_1	3.4	2.4
w_2	9.6	6

The EMF was computed using the Finite-Difference Time-Domain (FDTD) solver. Briefly, the FDTD method involves both a spatial and temporal discretization of the electric and magnetic fields over a period of time and a specific spatial domain limited with the boundary conditions. Typically, the minimum spatial sampling is of 10-20 per wavelength, and the temporal sampling is sufficiently small to maintain stability of the algorithm [29]. All the simulations were performed in the software platform Sim4Life v.7 (ZMT Zurich Med Tech AG, Zurich Switzerland, www.zmt.swiss, accessed on 9 February 2023).

The computational domain was discretized with an adaptive non-uniform grid for the antenna and the surrounding of the phantom with a sub-wavelength resolution of around 15 mesh cells per wavelength. We set the mesh cell size varying from 0.06 mm to 0.33 mm depending on the dielectric properties of the model, in order to correctly discretize all the tissues to guarantee the compliance with the constraint of $\lambda/10$ imposed by the FDTD method for its stability. This resulted in total in 8.537 and 162.310 MCells at 28 and 39 GHz, respectively. The computational domain was truncated by assuming 8 layers of perfectly matched layer (PML) material and 10 cells of free space were added around the computational domain at the domain boundaries.

The simulations were performed on a workstation Z8 16-Core Processor @3.8 GHz, RAM 512 GB, with a graphical card NVIDIA GeForce RTX5000. To speed up simulations, Sim4Life GPU accelerator aXware was used, and the maximum computational time was 30 minutes.

The Absorbed Power Density (S_{ab}, W/m^2) averaged over a surface of 1 cm^2 or 4 cm^2 of tissue was calculated as [20], [24], [25]:

$$S_{ab} = (1/A)\int\int_A \mathrm{Re}[\mathbf{E} \text{ x } \mathbf{H}^*]d\mathbf{S} \tag{1}$$

where A is the surface averaging area, d$\mathbf{S}$ is the surface element and Re [$\mathbf{E}$ x $\mathbf{H}^*$] is the real part of the Poynting vector, where **E** and **H** are inside the body surface and meant as root-mean-square values. Moreover, the power transmitted through the surface is determined by means of the computational integration of the power density over a surface area (A) within a square area entirely contained in A. With more details, the implemented algorithm for the estimation of the S_{ab} uses the rotating square as planar averaging surface.

As mentioned before, the IEEE Std C95.1 [21] specifies that the estimated power density must be calculated over the epithelial surface, i.e., the stratum corneum for the skin, conversely, the ICNIRP Guidelines [20] do not provide any specifications in this respect.

Moreover, according to the ICNIRP Guidelines [20] and the IEEE Std. C95.1 [21], the estimation of the S_{ab} averaged over 1 cm^2 is recommended above 30 GHz, since focal beam exposure can occur, whereas > 6 GHz the S_{ab} is to be averaged over 4 cm^2. However, since one of the frequencies faced in the present work is close to 30 GHz (i.e. 28 GHz), we have opted for the extraction of the S_{ab} averaged over both the 1 cm^2 and 4 cm^2 areas, for both frequencies.

D. ANALYTICAL APPROACH

All the tissue models described above were also exposed to TEM-polarized plane wave, and the reflection coefficient was calculated at the interface air/phantom following the generic formula (2) for a M-layer structure [30]:

$$\Gamma_i = (\rho_i + \Gamma_{i+1}e^{-2jk_il_i})/(1 + \rho_i\Gamma_{i+1}e^{-2jk_il_i}) \tag{2}$$

where $i = M, M - 1, \ldots 1$ and it is initialized by $\Gamma_{M+1} = \rho_{M+1}$. The absorbed power density (S_{ab}) is then retrieved using the formula (3) in the ICNIRP Guidelines [20]:

$$S_{ab} = (1 - |\Gamma|^2) \cdot S_{inc} \tag{3}$$

where S_{inc} is the incident power density set to 10 W/m^2, corresponding to the ICNIRP reference level for the general public (Table 5 in [20]).

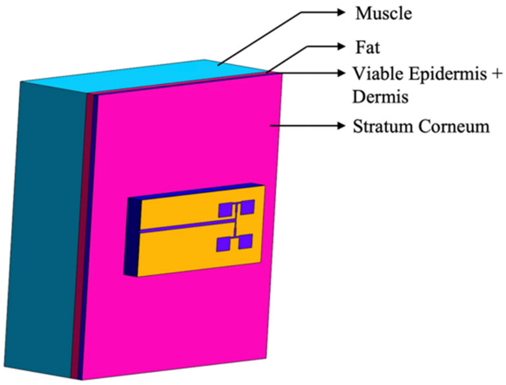

FIGURE 3. Example of simulated scenario with antenna positioned 2 mm away from the center of the skin model (for the sake of readability, the size of the phantom and antenna are not in scale).

III. RESULTS

This sections reports computed, and analytically calculated S_{ab} induced by on-body antennas in tissue-equivalent models of increasing complexity.

A. NUMERCIAL ANALYSIS

The computed peak values of the S_{ab} averaged over 1 cm^2 and 4 cm^2 with the accepted power of 100 mW are presented in Fig.4. Due to local exposure, for all models and tissues the peak S_{ab} averaged over 1 cm^2 (top row) is higher than the corresponding ones averaged over 4 cm^2 (bottom row). For the sake of brevity, the results that will be discussed hereafter are for S_{ab} averaged over a rotating square of 1 cm^2 but the trend is similar for S_{ab} averaged over a rotating square of 4 cm^2.

As reported in the upper left panel of Fig.4, the highest peak S_{ab} at 28 GHz is found in the SC of the 4-layer model i.e., 4.32 W/m^2. The maximum variation of peak S_{ab} in the SC in multi-layer models is around 3%. The lowest value is obtained for the 2-layer model, and it increases by crossing through 3- and 4-layer models. The exposure levels in epidermis and dermis layer are almost identical as well ($<$ 2.5% deviation) across multi-layer models. For fat the results showed a maximum variation of 8% across the 3- and 4-layer models. Furthermore, by passing through the layers from the outer to the inner one, the peak S_{ab} decreases, confirming that lowest values are always in the most internal stratum. The muscle, the fourth tissue in the 4-layer model, experienced negligible exposure reduced by roughly 97% with respect to maximum value in SC.

This comparison highlights that, for certain layer thicknesses of multi-layer models, the commonly used homogeneous dry skin model with Gabriel's properties [31] slightly underestimates the peak value of S_{ab} obtained in SC of the multi-layer models. Indeed, the peak S_{ab} obtained in the homogeneous model is reduced by 8.5% to 11%, with respect to the peak S_{ab} in SC of the multi-layer models. Similarly, from the comparison of the peak S_{ab} in the epidermis and dermis across all the models, the difference between the peak in the homogeneous model (i.e., 3.8 W/m^2) and the ones in the multi-layer models (i.e., 4.36 W/m^2, 4.3 W/m^2, and 4.26, W/m^2, from the 4- to the 2-layer models) is noteworthy.

The general trends observed at 39 GHz are similar to those at 28 GHz. First of all, the maximum peak is observed in the SC of the 4-layer model i.e., 4.85 W/m^2. Nevertheless, comparing this peak value with the ones of the 2- and 3-layer models there is no substantial differences (deviation $<$ 2%). The lowest peak S_{ab} is observed in the 2-layer model even if the comparison between the 4- and the 3-layer models did not reveal noteworthy variations ($<$1% deviation). Moreover, the peak S_{ab} in dermis across the 2-, 3- and 4-layer models are almost the same ($<$2% deviation), whereas in the fat the variation between the 3- and the 4-layer models revealed almost 4% of deviation.

Certainly, the trend of the decrease of the exposure levels from the outer to the inner tissues is amplified at a higher frequency; indeed the peak S_{ab} switches from 4.85 W/m^2 in SC down to 0.05 W/m^2 in muscle, showing S_{ab} reduction of 98.7%.

Furthermore, the comparison between the multi-layer models and the homogeneous model showed similar behavior at 28 GHz: the homogeneous model (4.24 W/m^2) tends to underestimate to some extent the S_{ab} with respect to the peaks estimated in the SC of the multi-layer model. More specifically, the deviation varies from 11% to the maximum of around 12.5%. Conversely, the results obtained in the dermis of the multi-layer models (i.e., 4.85 W/m^2, 4.83 W/m^2, and 4.76 W/m^2 in the 4-, 3-, and 2-layer model respectively) are almost the same, showing a maximum variation of 2%.

B. ANALYTICAL CALCULATIONS

In this section, the results on the peak S_{ab} analytically calculated for plane-wave exposure with the angle of incidence varying from 0° to 80° are presented. The incident power density (S_{inc}) is set to 10 W/m^2, corresponding to the ICNIRP reference level for the general public in the 2-300 GHz range [20].

Fig. 5 summarized the calculated peak S_{ab}as a function of angle of incidence. The results show that S_{ab} at the air/model interface in the homogeneous model does not noticeably differ from those obtained in the outermost layer of the multi-layer models. Comparing the results obtained in the homogeneous model to those in the multi-layer models, it can be stated that they are similar. The maximum deviation is approximately 5%, occurring in cases of the normal incidence at 39 GHz. In all other cases, differences are limited to 2%, and this trend is in line with the literature data [19]. Considering only the multi-layer models, the exposure levels are almost identical ($<$ 1% deviation across all the models for 28 GHz and for the 39 GHz). When comparing the results obtained for different frequencies, it is evident that the calculated absorbed power density values for a plane wave at 28 GHz are slightly lower than those calculated with a wave at 39 GHz, with a deviation of approximately 5%. This holds true for both the homogeneous

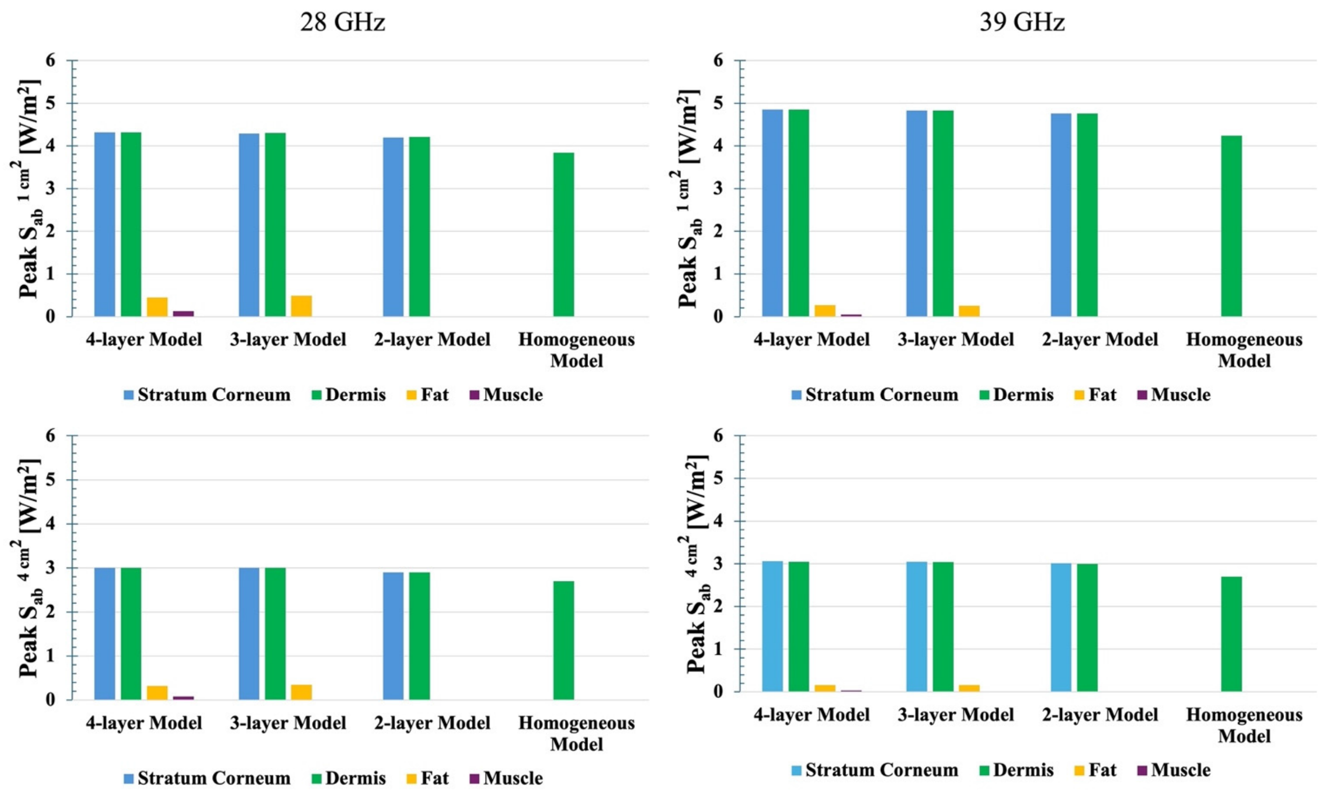

FIGURE 4. Peak spatial-averaged absorbed power density (S_{ab}) for different tissue-equivalent models.

model and the multi-layer models. This trend indicates that as the frequency increases, the absorbed power density also increases. Furthermore, this trend remains consistent across the considered range of the angles of incidence. Lastly, focusing on the comparison by propagation mode of the plane waves, the absorbed power density values are higher when the Incident wave is TM-polarized compared to when it is TE-polarized as expected, and this trend holds true for both analyzed frequencies, with variations ranging from 7% up to approximately 20%.

IV. DISCUSSION

Wearable wireless technologies are attractive for various communication and sensing applications, including personal healthcare, smart home, sport and so on. The healthcare has been the primary target application so far, however recently wearable communicating devices also demonstrated a potential for other usages such as military and entertainment [33]. The wearable devices may be a part of Wireless Body-Area Networks (WBAN) introduced in the IEEE 802.15.6 standard [5]. In WBAN, information deriving from the sensors is collected in a central unit and then transmitted to an external device (e.g., the smartphone) [4]. Recently, the wearable networks have also included 5G technology. Indeed, the use of the 5G protocol permits, for example, the possibility to involve augmented, mixed, and virtual realities [32]. For this reason, 5G bands are involved in wearable communication, particularly in the mmWaves band (>24 GHz).

Since wearable devices are positioned on the human body, the question of the power absorbed by human tissues is crucial and timely, particular if mmWave wearable antenna are considered. Indeed, only few studies (see as examples [33], [34], [35]) aimed to assess the exposure generated specifically by wearable antennas at 5G frequencies using both simplified that detailed anatomical human models. In particular, only one recent paper by Gallucci et al., [35], computationally assessed the human exposure due to the EMF emitted by wearable antennas, each one tuned to a 5G band (one to 3.5 GHz and the second one to 26.5 GHz), positioned on the trunk of four realistic human models of the Virtual Population [11].

However, to numerically characterize antenna/body interactions, the use of an appropriate tissue model is crucial as it directly impacts the accuracy of results. Indeed, particularly for mmWave frequencies up to 100 GHz, modelling the skin by a single layer of homogeneous dermis tissue with constant dielectric properties over its entire thickness, as it is done in the most popular anatomical models [12], could be an oversimplification to realistically represent the skin structure. As a consequence, stratified multi-layer models were introduced in literature [13], [14]. These models are typically composed of the stratum corneum, viable epidermis and dermis, fat, and

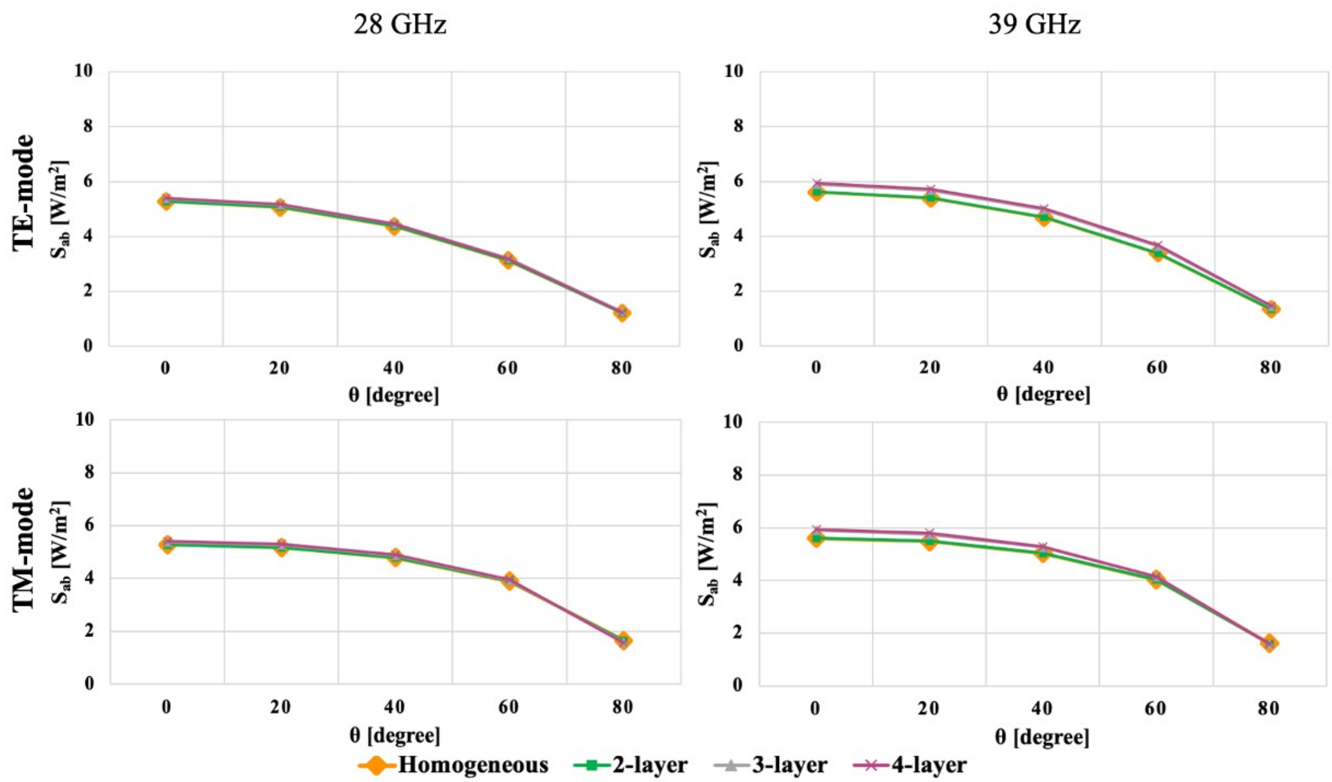

FIGURE 5. Peak values of the absorbed power density (S_{ab}) in the outermost tissue of the models as a function of angle of incidence (θ): TE polarization (first raw), TM polarization (second raw).

muscle. However, in literature there is not yet a consensus about the approach to employ in studies of computational exposure assessment to model the cutaneous tissue.

This work is inserted in this context, investigating the exposure levels induced by two wearable patch antennas tuned in the 5G bands, using models with different stratifications to investigate the impact that the choice of a multi-layer model rather than the homogeneous one has on the exposure assessment. Specifically, four planar models with increasing complexity were considered: from a homogeneous model with dermis properties to the four-layer model composed of thin SC, dermis, fat, and muscle. The exposure was quantified by the assessment of the S_{ab} averaged over both 1 cm^2 and 4 cm^2.

As mentioned before, the exposure scenarios were approached also analytically, by simulating the four human models irradiated by a plane wave at 28 GHz and 39 GHz. The numerical and analytical results indicated different trends: in case of analytical results where the source is a plane wave, the values of the S_{ab} calculated in the outermost surface at the air/model interface found in the homogeneous model are comparable with those found in the multi-layer models, while computational results with a physical antenna have highlighted a different trend, whereby the homogeneous model slightly (from 8% to 12%) underestimates the exposure levels with respect to the outermost layer of any of the multi-layer models. The reason of these minor discrepancies is in the simplification of the scenario that the analytical study provides, considering, for example, the simplification of the source becoming a plane wave, and the propagation mode of the wave that is not applicable to the EMF emitted by an antenna, even more if we consider the backscattering of the antenna because of its position with respect to the human model due to its way of use, as in the case of wearable devices. Finally, it is also important to underline that there is always a marginal error due to the approximation of the computational methods affecting the results. In order to quantify the discrepancy between computational results and those that would be obtained by approaching the complex scenario analytically, scenarios here faced using the analytical approach were also addressed computationally, using the same simulations software as for the wearable antennas. We found that the maximum deviation between the computational and the analytical results in the case of an impinging plane wave to the here simulated models, one at a time, is at most 8%, revealing a good matching between the analytical and the computational data.

As to the computational results with wearable antennas, analyzing the data of the peak value of the S_{ab} when the antenna is tuned to 28 GHz, it is observed that the use of the homogeneous dry skin model led to an underestimation of the exposure levels in the most external layer of the model with respect to the multi-layer models ranging from 8.5% to 11%, according to the 2-3- or 4-layer models. This trend is similar to the scenario with the antenna at 39 GHz showing an underestimation ranging from 11 % to 12.5%.

Furthermore, the grouping of these results by frequency shows the fact that the lower the frequency, the more noticeable the underestimation of the homogeneous model over the stratified models. This evidence is confirmed by the studies in literature, even though their number is limited. Firstly, Bonato et al. [36] computationally simulated the homogeneous, and the three- and four-layer models with thick SC in three different exposure configurations to a 5G mobile phone antenna at 27 GHz (by varying the distance antenna-user), showing that the homogeneous model tended to underestimate the exposure in all the scenarios. Sasaki et al. [37] used the Monte Carlo simulation approach with varying the tissue thicknesses of the exposed homogeneous and two-layer models with thin SC. All the planar multi-layer models were exposed to plane waves from 0.1 to 1 THz and with $S_{inc} = 1$ W/m^2. In their work, they demonstrated that, from 100 GHz up to 500 GHz, the power transmittance increases when the skin is deeper modeled, above 500 GHz the transmittance is saturated. Finally, Christ et al. [18] conducted a study in which incident plane waves at frequencies from 6 to 100 GHz impinged on several stratified most superficial tissue models. Here, the power transmission coefficient and the temperature increase were studied. This work highlighted the trend of underestimation of the temperature increase by the homogeneous dermis model with respect to the stratified one by more than a factor of three. In light of the aforementioned points, the majority of studies have found differences in power absorption levels with thin SC above 100 GHz, or at lower frequencies when the stratified model features a thick outer layer that characterizes only specific body districts, such as palm. However, concerning the typical positioning of wearable devices, the stratified model made more sense if it was modelled with the thin outer tissue layer, a model for which differences in power absorption levels had not been found when it is compared to the homogeneous model thus far. It is also true, though, that the studies in question involved the use of plane waves, which is a simplification compared to realistic electromagnetic sources. In our study, by combining the stratified skin model with thin SC and a complex antenna, we found differences in terms of exposure levels between the stratified and homogeneous models. These findings, however, are in line with the definition of the epithelial power density given in IEEE Std. C95.1 [21] recommending the estimation of power density at the level of the stratum corneum to obtain more reliable values. Comparing the responses of the different multi-layer models, our data suggested that there are no substantial differences between the multi-layer models, particularly for the most external layer. In this regard, it was found that for the scenario with the lowest frequency the maximum variation of S_{ab} is of 8% and it was between the four- and the three-layer models, precisely in the fat, whereas the greatest variation in the SC is of almost 3% between the two- and the four-layer models. This means that, at this frequency, choosing a stratified model rather than another always structured, the maximum expected impact on the exposure is 8%, particularly in the inner layer. For what concern the 39 GHz scenario, this maximum variation resides again in the fat, and it is almost 4%, reducing the impact that the choice of a certain stratified model has on the exposure assessment, whereas for the outer strata the variation is almost 2%.

Finally, the comparison of the values reported in the left column with the peaks in the right column of Fig.4 showed that the peaks in the inner tissues (i.e., muscle) assessed in the scenario with the lowest frequency are higher than the peaks S_{ab} observed at 39 GHz. Indeed, the difference between the peaks with the antenna at 28 GHz and the ones with 39 GHz is more evident in the inner strata rather than the outer layers so much so that the variation in the SC is of 10.9%, whereas in the muscle it is 61.5%. This is in line with the decrease of the penetration depth corresponding to the increase of the frequency.

Overall, from the comparison with the ICNIRP Guidelines [20], in any of the studied configurations the limit of 20 W/m^2 has not been exceeded on the interface air/skin when the input power to the antenna is the typical one for the wearable antennas. On the other hand, the question about the lack of a formal definition of the best model to simulate the cutaneous tissue is still open. In the international regulations there is no specific information about the model that well reproduces the skin. This is a real gap in the exposure assessment procedure because, as shown in this paper and in the literature, the exposure levels are slightly different depending on the chosen model and further investigations are still useful in order to have a clear picture about the consequences that the choice of a model implies in the exposure assessment results, especially when an actual EMF source is involved.

V. CONCLUSION

In conclusion, the present work aimed to assess the exposure to two mmWave wearable antennas using four tissue-equivalent models of increasing complexity to investigate their effect on the exposure level.

The numerical results demonstrated that, the peak S_{ab} in the homogeneous model is always modestly lower than the ones in the layered models with the same reflection coefficient. This finding suggests that the use of the homogeneous skin model in exposure assessment studies with wearable antennas tuned to high frequencies may underestimate the exposure, compared to the stratified skin models where the inner structure of the cutaneous tissue is taken into account. This trend has not been observed in the analytical results with plane wave as source where the differences in the S_{ab} across all the models are more limited. In the literature the number of studies facing this issue is restricted; moreover it is important to underline that here each skin layer was modelled with a precise thickness kept coherent in all the simulations even though each stratum thickness varies in a range depending on some factors such as the anatomical region and the body's conditions of the user; this limit could be overcome through the employment of the high-detailed virtual human models having the geometry of each tissue more detailed in order to identify the extent to which the choice to the simplified geometry of the model could impact on the results.

In light of these considerations, further investigations are needed in order to generalize more these interesting and impactful results.

ACKNOWLEDGMENT

The authors wish to thank ZMT Zurich MedTech AG (www.zmt.swiss, accessed on 1st February 2024) for having provided the simulation software Sim4Life.

REFERENCES

[1] K. N. Paracha, S. K. Abdul Rahim, P. J. Soh, and M. Khalily, "Wearable antennas: A review of materials, structures, and innovative features for autonomous communication and sensing," *IEEE Access*, vol. 7, pp. 56694–56712, 2019.

[2] H. Lee, J. Tak, and J. Choi, "Wearable antenna integrated into military berets for indoor/outdoor positioning system," *IEEE Antennas Wireless Propag. Lett.*, vol. 16, pp. 1919–1922, 2017.

[3] R. Punj and R. Kumar, "Technological aspects of WBANs for health monitoring: A comprehensive review," *Wireless Netw.*, vol. 25, no. 3, pp. 1125–1157, Apr. 2019.

[4] M. Chen, S. Gonzalez, A. Vasilakos, H. Cao, and V. C. M. Leung, "Body area networks: A survey," *Mobile Netw. Appl.*, vol. 16, no. 2, pp. 171–193, 2011.

[5] *IEEE Standard for Local and Metropolitan Area Networks—Part 15.6: Wireless Body Area Networks*, IEEE Standard 802.15.6, 2012.

[6] R. Gravina and G. Fortino, "Wearable body sensor networks: State-of-the-art and research directions," *IEEE Sensors J.*, vol. 21, no. 11, pp. 12511–12522, Jun. 2021.

[7] A. Hirata, Y. Diao, T. Onishi, K. Sasaki, S. Ahn, D. Colombi, V. De Santis, I. Laakso, L. Giaccone, W. Joseph, E. A. Rashed, W. Kainz, and J. Chen, "Assessment of human exposure to electromagnetic fields: Review and future directions," *IEEE Trans. Electromagn. Compat.*, vol. 63, no. 5, pp. 1619–1630, Oct. 2021.

[8] M. Ur-Rehman, M. Adekanye, and H. T. Chattha, "Tri-band millimetre-wave antenna for body-centric networks," *Nano Commun. Netw.*, vol. 18, pp. 72–81, Dec. 2018.

[9] U. Farooq and G. M. Rather, "A miniaturised Ka/V dual band millimeter wave antenna for 5G body centric network applications," *Alexandria Eng. J.*, vol. 61, no. 10, pp. 8089–8096, Oct. 2022.

[10] C. Leduc and M. Zhadobov, "Impact of antenna topology and feeding technique on coupling with human body: Application to 60-GHz antenna arrays," *IEEE Trans. Antennas Propag.*, vol. 65, no. 12, pp. 6779–6787, Dec. 2017.

[11] M.-C. Gosselin, E. Neufeld, H. Moser, E. Huber, S. Farcito, L. Gerber, M. Jedensjö, I. Hilber, F. D. Gennaro, B. Lloyd, E. Cherubini, D. Szczerba, W. Kainz, and N. Kuster, "Development of a new generation of high-resolution anatomical models for medical device evaluation: The virtual population 3.0," *Phys. Med. Biol.*, vol. 59, no. 18, pp. 5287–5303, Sep. 2014.

[12] W. Kainz, E. Neufeld, W. E. Bolch, C. G. Graff, C. H. Kim, N. Kuster, B. Lloyd, T. Morrison, P. Segars, Y. S. Yeom, M. Zankl, X. G. Xu, and B. M. W. Tsui, "Advances in computational human phantoms and their applications in biomedical engineering—A topical review," *IEEE Trans. Radiat. Plasma Med. Sci.*, vol. 3, no. 1, pp. 1–23, Jan. 2019.

[13] M. C. Ziskin, S. I. Alekseev, K. R. Foster, and Q. Balzano, "Tissue models for RF exposure evaluation at frequencies above 6 GHz," *Bioelectromagnetics*, vol. 39, no. 3, pp. 173–189, Apr. 2018.

[14] S. I. Alekseev and M. C. Ziskin, "Human skin permittivity determined by millimeter wave reflection measurements," *Bioelectromagnetics*, vol. 28, no. 5, pp. 331–339, Jul. 2007.

[15] S. I. Alekseev, A. A. Radzievsky, M. K. Logani, and M. C. Ziskin, "Millimeter wave dosimetry of human skin," *Bioelectromagnetics*, vol. 29, no. 1, pp. 65–70, Jan. 2008.

[16] K. Sasaki, M. Mizuno, K. Wake, and S. Watanabe, "Monte Carlo simulations of skin exposure to electromagnetic field from 10 GHz to 1 THz," *Phys. Med. Biol.*, vol. 62, no. 17, pp. 6993–7010, Aug. 2017.

[17] G. Sacco, S. Pisa, and M. Zhadobov, "Age-dependence of electromagnetic power and heat deposition in near-surface tissues in emerging 5G bands," *Sci. Rep.*, vol. 11, no. 1, p. 3983, Feb. 2021.

[18] A. Christ, T. Samaras, E. Neufeld, and N. Kuster, "RF-induced temperature increase in a stratified model of the skin for plane-wave exposure at 6–100 GHz," *Radiat. Protection Dosimetry*, vol. 188, no. 3, pp. 350–360, Jun. 2020.

[19] A. Christ, T. Samaras, E. Neufeld, and N. Kuster, "Transmission coefficient of power density into skin tissue between 6 and 300 GHz," *Radiat. Protection Dosimetry*, vol. 192, no. 1, pp. 113–118, Dec. 2020.

[20] ICNIRP, "Guidelines for limiting exposure to electromagnetic fields (100 kHz to 300 GHz)," *Health Phys.*, vol. 118, no. 5, pp. 483–524, 2020.

[21] *IEEE Standard for Safety Levels With Respect to Human Exposure to Electric, Magnetic, and Electromagnetic Fields, 0 Hz to 300 GHz*, Standard C95.1-2019, 2019, pp. 1–312.

[22] T. Samaras, A. Christ, and N. Kuster, "Compliance assessment of the epithelial or absorbed power density below 10 GHz using SAR measurement systems," *Bioelectromagnetics*, vol. 42, no. 6, pp. 484–490, Sep. 2021.

[23] S. S. Zhekov, M. Yao, C. D. Paola, B. Xu, and S. Zhang, "A study on EMF exposure assessments with different metrics for user equipment antennas at 6 and 10 GHz," *IEEE Trans. Electromagn. Compat.*, vol. 66, no. 1, pp. 61–69, Feb. 2024.

[24] K. Li, S. Kodera, D. Poljak, Y. Diao, K. Sasaki, A. Šušnjara, A. Prokop, K. Taguchi, J. Xi, S. Zhang, M. Yao, G. Sacco, M. Zhadobov, W. E. Hajj, and A. Hirata, "Calculated epithelial/absorbed power density for exposure from antennas at 10–90 GHz: Intercomparison study using a planar skin model," *IEEE Access*, vol. 11, pp. 7420–7435, 2023.

[25] K. Li, S. Kodera, D. Poljak, Y. Diao, K. Sasaki, S. Zhang, M. Yao, A. Kapetanovic, C. Li, T. Wu, T. Liebig, W. Simon, and A. Hirata, "Spatially averaged epithelial/absorbed power density for nonplanar skin models exposed to antenna at 10–90 GHz," *IEEE Access*, vol. 12, pp. 15379–15389, 2024.

[26] A. L. Kapetanovic, G. Sacco, D. Poljak, and M. Zhadobov, "Area-averaged transmitted and absorbed power density on a realistic ear model," *IEEE J. Electromagn., RF Microw. Med. Biol.*, vol. 7, no. 1, pp. 39–45, Mar. 2023.

[27] R. Poonkuzhali, Z. C. Alex, and T. N. Balakrishnan, "Miniaturized wearable fractal antenna for military applications at VHF band," *Prog. Electromagn. Res. C*, vol. 62, pp. 179–190, 2016.

[28] N. Chahat, M. Zhadobov, L. Le Coq, S. I. Alekseev, and R. Sauleau, "Characterization of the interactions between a 60-GHz antenna and the human body in an off-body scenario," *IEEE Trans. Antennas Propag.*, vol. 60, no. 12, pp. 5958–5965, Dec. 2012.

[29] J. W. Hand, "Modelling the interaction of electromagnetic fields (10 MHz–10 GHz) with the human body: Methods and applications," *Phys. Med. Biol.*, vol. 53, no. 16, pp. R243–R286, Aug. 2008.

[30] S. Ramo, J. R. Whinnery, and T. Van Duzer, *Fields and Waves in Communication Electronics*. Hoboken, NJ, USA: Wiley, 1994.

[31] S. Gabriel, R. W. Lau, and C. Gabriel, "The dielectric properties of biological tissues: III. Parametric models for the dielectric spectrum of tissues," *Phys. Med. Biol.*, vol. 41, no. 11, pp. 2271–2293, Nov. 1996.

[32] A. Ometov, V. Shubina, L. Klus, J. Skibinska, S. Saafi, P. Pascacio, L. Flueratoru, D. Q. Gaibor, N. Chukhno, O. Chukhno, and A. Ali, "A survey on wearable technology: History, state-of-the-art and current challenges," *Comput. Netw.*, vol. 193, Jul. 2021, Art. no. 108074.

[33] E. M. Wissem, I. Sfar, L. Osman, and J.-M. Ribero, "A textile EBG-based antenna for future 5G-IoT millimeter-wave applications," *Electronics*, vol. 10, no. 2, p. 154, Jan. 2021.

[34] C. Du, X. Li, and S. Zhong, "Compact liquid crystal polymer based tri-band flexible antenna for WLAN/WiMAX/5G applications," *IEEE Access*, early access, Jun. 4, 2024, doi: 10.1109/ACCESS.2019.2941212.

[35] S. Gallucci, M. Bonato, M. Benini, E. Chiaramello, S. Fiocchi, G. Tognola, and M. Parazzini, "Assessment of EMF human exposure levels due to wearable antennas at 5G frequency band," *Sensors*, vol. 23, no. 1, p. 104, Dec. 2022.

[36] M. Bonato, L. Dossi, S. Gallucci, M. Benini, G. Tognola, and M. Parazzini, "Assessment of human exposure levels due to mobile phone antennas in 5G networks," *Int. J. Environ. Res. Public Health*, vol. 19, no. 3, p. 1546, Jan. 2022.

[37] K. Sasaki, K. Li, and T. Nagaoka, "Human skin exposure to terahertz waves from 0.1 to 1 THz: Statistical assessments using multilayered planar models," in *IEEE MTT-S Int. Microw. Symp. Dig.*, Suzhou, China, May 2022, pp. 25–27.

SILVIA GALLUCCI received the master's degree in biomedical engineering from the University of Pisa, Italy, in 2019, and the Ph.D. degree in bioengineering from Politecnico di Milano, with a focus on the EMF interactions. Since January 2024, she has been a Research Scientist with the Institute of Electronics, Computer and Telecommunication Engineering, Consiglio Nazionale delle Ricerche. Her research interest includes the exposure assessment of electromagnetic fields with numerical dosimetry, particularly from 5G mobile communications.

MARTA BONATO received the master's and Ph.D. degrees in biomedical engineering from the Polytechnic University of Milan, Milan, Italy, in 2017 and 2021, respectively. From May 2021 to February 2024, she was with the Institute of Electronics, Computer and Telecommunication Engineering, Consiglio Nazionale delle Ricerche, Italy, as a Researcher Scientist. Her current research interests include the study of the interaction of electromagnetic fields (EMF) with biological systems and the study of possible effects of EMF on health with both deterministic and stochastic dosimetry, particularly from 5G mobile communications.

MARTINA BENINI received the B.S. degree in biomedical engineering from Alma Mater Studiorum—Università di Bologna, Italy, in 2017, and the M.S. degree in biomedical engineering from Politecnico di Milano, Italy, in 2020, where she is currently pursuing the Ph.D. degree in bioengineering. From October 2020 to April 2021, she was a Research Fellow with the Institute of Electronics, Information Engineering and Telecommunications (IEIIT), Consiglio Nazionale delle Ricerche (CNR). Her current research interests include the study of the interaction between the electromagnetic fields (EMFs) and the human body with both deterministic and stochastic dosimetry, with a focus on the antennas used in the automotive field for vehicular connectivity.

MARTA PARAZZINI (Member, IEEE) is currently a Senior Researcher with the Institute of Electronics, Computer, and Telecommunication Engineering (IEIIT), Consiglio Nazionale Delle Ricerche, Rome, Italy. Her current research interests include the study of the interactions of EMF with biological systems, deterministic and stochastic computational dosimetry, and the medical applications of EMF, in particular the techniques for noninvasive brain stimulation.

MAXIM ZHADOBOV (Senior Member, IEEE) received the Ph.D. and Habilitation á Diriger des Recherches degrees from the Institut d'Electronique et des Technologies du numéRique (IETR), University of Rennes 1, Rennes, France, in 2006 and 2016, respectively. He was a Postdoctoral Researcher with the Center for Biomedical Physics, Temple University, Philadelphia, PA, USA, until 2008, and then joined the French National Center for Scientific Research (CNRS). He is currently a Senior Research Scientist with the IETR/CNRS in charge of the Electromagnetic Waves in Complex Media (eWAVES) Research Group. He was also on review boards of more than 15 international journals and conferences, and has been acting as an expert at research councils worldwide. He has coauthored five book chapters, 85 research articles in peer-reviewed international journals, and more than 200 contributions to conferences and workshops. His review article in the *International Journal of Microwave and Wireless Technologies* has been the most cited paper since 2016. A paper published by his research group, in 2019, is in journal Top 100 of *Scientific Reports* (Nature). He has been involved in 26 research projects (14 as a PI). His research interests include innovative biomedical applications of electromagnetic fields and associated technologies. He was the TPC member and/or session organizer at international conferences, including AES 2023, EUMW2022, IEEE IMBioC 2022, AT-AP-RASC 2022, BioEM 2019, EuMW 2019, IEEE iWEM 2017, MobiHealth 2015–2017, BodyNets 2016, and IMWS-Bio 2014. He was an Elected Member of EBEA Council, from 2017 to 2021. He is a member of IEEE TC95.4. He was a recipient of the Research and Innovation Award from BPGO, in 2022, the CNRS Medal, in 2018, the EBEA Award for Excellence in Bioelectromagnetics, in 2015, and the Brittany's Young Scientist Award, in 2010. Since 2010, the Ph.D. students he worked with have been recipients of seven national scientific awards and six awards from the Bioelectromagnetics Society, URSI, IEEE Antennas and Propagation Society, and IEEE Microwave Theory and Technology Society. He was the TPC Co-Chair of BioEM 2021/2020. He is currently the President of URSI France Commission K. He is an Associate Editor of IEEE Journal of Electromagnetics, RF and Microwaves in Medicine and Biology. He served as a Guest Editor for several special issues, including Human Exposure in 5G and 6G Scenarios of *Applied Sciences* and Advanced Electromagnetic Biosensors for Medical, Environmental and Industrial Applications of *Sensors*.

Open Access funding provided by 'Consiglio Nazionale delle Ricerche-CARI-CARE-ITALY' within the CRUI CARE Agreement